The Astrophysical Journal, 838:54 (10pp), 2017 March 20 https://doi.org/10.3847/1538-4357/aa6331

Relative Orbit Orientation in Several Resolved Multiple Systems

Andrei Tokovinin[1] and David W. Latham[2]
[1] Cerro Tololo Inter-American Observatory, Casilla 603, La Serena, Chile; atokovinin@ctio.noao.edu
[2] Harvard-Smithsonian Center for Astrophysics, 60 Garden Street, Cambridge, MA 02138, USA; dlatham@cfa.harvard.edu
Received 2016 December 13; revised 2017 February 24; accepted 2017 February 24; published 2017 March 23

Abstract

This work extends the still modest number of multiple stars with known relative orbit orientation. Accurate astrometry and radial velocities are used jointly to compute or update outer and inner orbits in three nearby triple systems, HIP 101955 (orbital periods 38.68 and 2.51 years), HIP 103987 (19.20 and 1.035 years), HIP 111805 (30.13 and 1.50 years), and in one quadruple system, HIP 2643 (periods 70.3, 4.85, and 0.276 years), all composed of solar-type stars. The masses are estimated from the absolute magnitudes and checked using the orbits. The ratios of outer to inner periods (from 14 to 20) and the eccentricities of the outer orbits are moderate. These systems are dynamically stable, but not very far from the stability limit. In three systems, all orbits are approximately coplanar and have small eccentricity, while in HIP 101955 the inner orbit with $e = 0.6$ is highly inclined.

Key words: binaries: general – binaries: spectroscopic – stars: solar-type

Supporting material: machine-readable tables

1. Introduction

Orbits of planets in the solar system, as well as in many exoplanet systems (Fabrycky et al. 2014), are located in one plane, presumably the plane of the protoplanetary disk. Some multiple stellar systems (e.g., HD 91962, Tokovinin et al. 2015) have a similar "planetary" architecture and could also be formed in a disk. However, this is not the universal rule. There are triple stars with nearly perpendicular orbits, like Algol, or even counter-rotating triple systems like ζ Aqr (Tokovinin 2016b). Similarly, there exist non-coplanar exoplanetary systems such as ν And (McArthur et al. 2010) and close binaries with misaligned stellar spins (Albrecht et al. 2014). Dynamical interactions with other stars or planets are often evoked to explain the misalignment. In very tight stellar systems, such interactions must be internal (between members) rather than external (with other stars in the cluster). Accretion of gas with random angular momentum during star formation is another promising, but poorly explored mechanism of misalignment.

Orbit orientation in triple stars provides observational constraints on the angular momentum history relevant to the formation of stellar systems, stars, and planets. However, the measurement of relative orbit orientation in triple stars is challenging. Both orbits must be resolved (either directly or astrometrically), the sense of rotation must be inferred from the radial velocities (RVs), and the outer period must not be too long for a reasonable orbit coverage. These conditions are met only for a small number of nearby multiple systems. The Sixth Catalog of Visual Binary Orbits (Hartkopf et al. 2001, VB6) contains 62 candidates of varying orbit quality, mostly without RV data. Without thorough re-assessment and filtering, the VB6 sample is not suitable for statistical study of relative orbit orientation. Long-baseline stellar interferometers help in resolving closer and faster subsystems, but require substantial efforts, contributing, so far, only a handful of cases (e.g., Kervella et al. 2013; Schaefer et al. 2016).

Motion in a triple system can be described by two Keplerian orbits only approximately because dynamical interaction between the inner and outer subsystems constantly changes their orbits. The timescale of this evolution is normally much longer than the time span of the observations, so the orbits represent the "instantaneous" osculating elements in the three-body problem. Knowing these orbits and the masses, the secular dynamical evolution can be studied numerically (Xu et al. 2015).

In this work, we study four multiple systems to determine their relative orbit orientation and period ratio as accurately as possible. We selected candidates with modest period ratios and moderate outer eccentricity, resembling in this sense HD 91962. Integer period ratios would suggest potential mean motion resonances. Such resonances are commonly found in multi-planet systems (Fabrycky et al. 2014), but are not documented in stellar multiples; the case of HD 91962 with a period ratio of 18.97 ± 0.06 remains, so far, unique (see however Zhu et al. 2016).

Basic data on the four multiple systems are presented in Table 1; the mobile diagrams in Figure 1 illustrate their hierarchical structure and periods. The range of periods is similar to that in the solar system. The last two columns of the table give the parallax from van Leeuwen (2007) and the dynamical parallax computed here from the orbital elements and estimated masses. HIP 2643 is a known visual binary containing two spectroscopic subsystems (hence it is quadruple); we detect here astrometric perturbations from the five-year subsystem. The remaining three triple stars have both inner and outer pairs directly resolved, with their orbits already listed in the VB6. HIP 103987 and 111805 were recently studied by Horch et al. (2015, hereafter H15). We use the available astrometry together with the new speckle observations and the RVs to compute combined orbits, accounting also for the "wobble" in the motion of the outer binary caused by the subsystem.

Section 2 presents the data used in this work and the methods common to all objects. Then each multiple system is discussed individually in Sections 3–6. The work is summarized in Section 7.

Table 1
Basic Parameters of Multiple Systems

HIP	HD	WDS (J2000)	Spectral type	V (mag)	$B-V$ (mag)	K (mag)	$\pi_{\rm HIP2}$ (mas)	$\pi_{\rm dyn}$ (mas)
2643	2993	00334+4006	F8	7.75	0.52	6.35	17.53 ± 0.95	16.1
101955	196795	20396+0458	K5V	7.84	1.24	4.74	59.80 ± 3.42	59.0
103987	200580	21041+0300	F9V	7.31	0.54	5.79	19.27 ± 0.99	23.2
111805	214608	22388+4419	F9V	6.83	0.55	5.32	26.18 ± 0.60	24.1

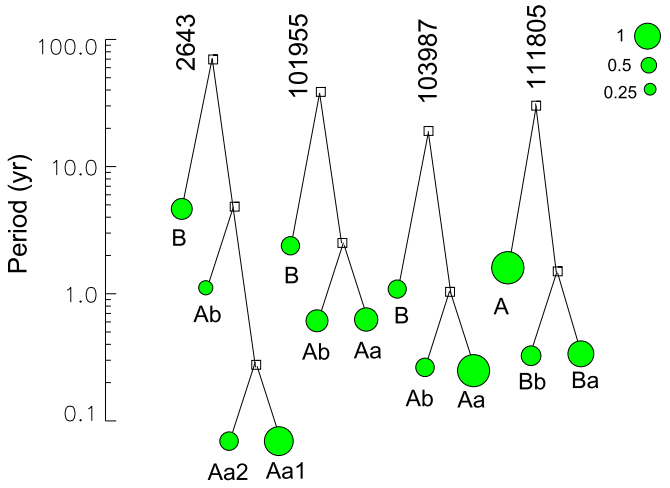

Figure 1. Mobile diagrams of four multiple systems. Squares denote the systems (period scale on the left), green circles—stars, with the circle diameter approximately proportional to the mass.

2. Observations and Their Analysis

2.1. Astrometry

The outer subsystems are classical visual binaries. Historic micrometric measurements and modern speckle interferometric data have been obtained from the WDS database on our request. Additionally, we secured new speckle astrometry and relative photometry of two systems at the 4.1 m SOAR telescope (Tokovinin et al. 2016). Accurate modern astrometry reveals "wobble" in the motion of the outer pairs caused by the subsystems, even when those are not directly resolved. The 180° ambiguity of position angle in the standard speckle method is avoided in the case of triple systems, where the orientation of the outer pair is known from micrometer measures and *Hipparcos* and defines the orientation of the inner pair as well. The observations presented in H15 use the image reconstruction technique that does not have the 180° ambiguity.

2.2. Radial Velocities

Published RVs are used here together with the new data. The RVs were measured with the CfA Digital Speedometers (Latham 1985, 1992), initially using the 1.5 m Wyeth Reflector at the Oak Ridge Observatory in the town of Harvard, Massachusetts, and subsequently with the 1.5 m Tillinghast Reflector at the Whipple Observatory on Mount Hopkins, Arizona. Starting in 2009, the new fiber-fed Tillinghast Reflector Echelle Spectrograph (TRES; Szentgyorgyi & Furész 2007) was used. The spectral resolution was 44,000 for all three spectrographs, but the typical signal-to-noise ratio per resolution element of 100 for the TRES observations was a few times higher than for the CfA Digital Speedometer observations.

The light of all systems except HIP 111805 is dominated by the bright primary component. Therefore, we followed our standard procedure of using one-dimensional correlations of each observed spectrum against a synthetic template drawn from our library of calculated spectra. The RV zero point for each spectrograph was monitored using observations of standard stars, of daytime sky, and of minor planets, and the velocities were all adjusted to the native system of the CfA Digital Speedometers. To get onto the absolute velocity system defined by our observations of minor planets, about 0.14 km s^{-1} should be added to the RVs. These velocities are all based on correlations of just a single echelle order centered on the Mg b triplet near 519 nm, with a wavelength window of 4.5 nm for the CfA Digital Speedometers and 10.0 nm for TRES.

Two objects, HIP 101955 and 103987, were observed in 2015 with the CHIRON echelle spectrograph (Tokovinin et al. 2013) at the 1.5 m telescope at CTIO with a spectral resolution of 80,000. The RVs were measured by cross-correlation of these spectra with the digital mask; see (Tokovinin 2016a) for further details.

2.3. Orbit Calculation

The orbital elements and their errors were determined with the IDL code `orbit3.pro`[3] that simultaneously fits the inner and outer orbits using both the resolved measures and the RVs. It describes the triple system "from inside out," as the first inner pair Aa,Ab and the second outer pair A,B, where A denotes the center of mass of Aa,Ab. The motion of the inner pair depends on the 10 inner elements. As the center of mass A moves in the outer orbit, the RVs of Aa and Ab are sums of the inner and outer orbital velocities, while the RV of B depends only on the outer elements. For the positional measurements, the situation is reversed: the position of the inner pair depends only on the inner elements, while the position of the outer pair includes the wobble term.

Figure 2 explains the wobble. The outer elements describe the motion of B around the center of mass A. However, the center of mass is not directly observed. Instead, the measurements of the outer pair give the vector Aa,B if the subsystem is resolved or refer to the photo-center A*,B otherwise. The primary Aa moves around the center of mass with an amplitude reduced by the wobble factor $f = q_1/(1+q_1)$ compared to the inner separation Aa,Ab, where q_1 is the inner mass ratio. For the photo-center, the appropriate wobble factor becomes $f^* = f - r_1/(1+r_1)$, where r_1 is the light ratio in the inner pair. The apparent trajectory of Aa,B or A*,B includes the wobble, it is not a closed ellipse.

[3] The code is posted at http://doi.org/10.5281/zenodo.321854.

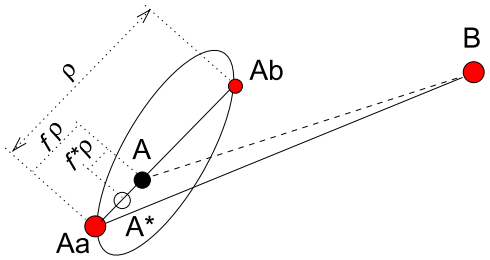

Figure 2. Scheme of a resolved triple star with the inner pair Aa,Ab and the outer pair A,B. Red circles denote stars, the black circle is the center of mass A, and the empty circle is the photo-center A*.

The 20 orbital elements (10 inner and 10 outer) are given as input to the program and then corrected iteratively to reach the χ^2 minimum. Errors of the positional measures are assumed to be isotropic (transverse equals radial). The errors of position measurements and RVs are balanced when the condition $\chi^2/M \sim 1$ is reached for each data set, where M is the number of degrees of freedom. Errors of the outliers are increased to reach this balance. The common systemic velocity V_0 is ascribed to the outer system (element 20), while the wobble factor f is stored as the element number 10. Currently, the code uses only one common wobble factor for all measures of the outer pair.

In two objects, HIP 2643 and HIP 103987, the inner subsystem is either unresolved or has questionable measures. The orientation of the inner orbit is then found only by modeling the wobble. In such cases, the inner semimajor axis a_1 and the wobble factor f cannot be determined separately. We have chosen to fix a_1 to its estimated value, while the wobble amplitude is still fitted freely through f.

When the tertiary component is brighter than the inner subsystem (it is usually denoted then as A), it is still considered to be a "tertiary" by the code. In such cases, the wobble factor f is negative and the outer elements Ω_2 and ω_2 are flipped by 180°.

The orbital elements and their errors are listed in Table 2. Its first column identifies each subsystem by the *Hipparcos* number and, in the following line, by the "discoverer code" and component designations joined by the comma. The following columns give the period P, the epoch of periastron T_0, the eccentricity e, the semimajor axis a, the position angle of the ascending node Ω_A (for the epoch J2000) and the argument of periastron ω_A (both angles refer to the primary component), the orbital inclination i, and the RV amplitudes K_1 and K_2. The last column contains the systemic velocity V_0 for the outer orbit and the wobble factor f for the inner orbit.

Table 3, available in full electronically, lists the positional measures and their residuals. Its first two columns identify the pair by its *Hipparcos* number and the system designation. The following columns contain (3) the date of observation in Besselian years, (4) the position angle θ, (5) the separation ρ, (6) the assumed error σ, (7) residual to the orbit in angle and (8) in separation. The last column (9) indicates the measurement technique, as described in the notes to the Table. Table 4, also available in full electronically, contains the RVs. Its first two columns specify the *Hipparcos* number and the component. Then follow (3) the Julian date, (4) the RV, (5) its error, and (6) the residual. The last column (7) gives the source of the RV, as explained in the notes.

2.4. Photometry and Masses

The relative photometry of the resolved pairs is available from *Hipparcos* and speckle interferometry. This defines the individual magnitudes of the components and, knowing the distance, their absolute magnitudes. All components are normal main-sequence stars, allowing us to estimate their masses from the standard relations. We use here the polynomial approximation of the absolute magnitude dependence on mass and wavelength from Tokovinin (2014). The magnitudes, distance, and masses constitute the model of each object (Table 5). Magnitudes not measured directly are given in brackets.

The sum of the estimated masses does not always match the mass sum computed from the orbital elements and the *Hipparcos* parallax. The latter can be biased by the complex orbital motion in multiple systems that has not been accounted for in the original *Hipparcos* data reduction (Söderhjelm 1999). Therefore, the distances used here are derived from the mass sum and the orbits (so-called dynamical parallaxes π_{dyn}, see Table 1). The RV amplitudes are used as a check, with the caveat of a potential RV bias due to blending with other components. The wobble amplitude and the combined color of the system are additional ways to check the consistency of the system models. For all multiple systems studied here, the minor discrepancies between various estimates of masses and magnitudes can be explained by the errors and biases.

3. HIP 2643

HIP 2643 (HD 2993) is known as a visual binary HO 3 or ADS 463. It has been first resolved in 1887 by Holden, so the measures cover 1.8 outer periods. The visual orbits of A,B were computed by several authors; the latest orbit by Mason & Hartkopf (2014) has $P = 69.15$ years. Independently, D. L. has discovered the RV variations with periods of 100 and 1485 days, meaning that the primary component is a spectroscopic triple, though only one star is seen in the spectra. The whole system is, therefore, a 3+1 quadruple with a 3-tier hierarchy, like HD 91962. The innermost 101 day pair is Aa1,Aa2, the middle pair is Aa,Ab, and the outer visual pair is A,B (Figure 1).

Accurate speckle measures of A,B available since 1985 allow us to detect the "wobble" caused by the middle subsystem Aa,Ab and to determine the elements of its astrometric orbit (Figure 3). Because our code cannot deal with quadruple stars, we first fitted the two inner spectroscopic orbits (the latest RVs were reduced by 1 km s^{-1} to account for the outer orbit). Then the RV variations caused by the 101-day inner orbit were subtracted, and the corrected RVs were used jointly with the positional measurements to fit the middle and outer orbits. Because there are no resolved measures of the middle subsystem, its semimajor axis was estimated from the masses and period and fixed to 58 mas, while the wobble factor f was fitted.

Although only two stars are directly observed, we can evaluate the masses of all four components. To begin with, we assume that the innermost orbit has a large inclination (this is justified in the following paragraph).[4] Then the inner RV amplitude and the estimated mass of Aa1 lead to the mass of Aa2, 0.36 $\mathcal{M}_\odot$. The inclination of the middle orbit is known, hence the mass of Ab is 0.42 $\mathcal{M}_\odot$, while the mass of B is

[4] We do not determine the orientation of the inner orbit in this paper.

Table 2
Orbital Elements

HIP/System Other Designation	P (year)	T_0 (year)	e	a ($''$)	Ω_A ($^\circ$)	ω_A ($^\circ$)	i ($^\circ$)	K_1 (km s^{-1})	K_2 (km s^{-1})	V_0, f (km s^{-1})
2643/outer	70.34	1983.62	0.331	0.393	118.9	137.8	112.3	(3.2)	(6.9)	−1.37
HO 3 A,B	±1.36	±0.60	±0.032	±0.020	±0.5	±2.7	±0.9	…	…	±0.19
2643/middle	4.849	1994.927	0.138	(0.058)	100.7	132.3	94.0	4.857	…	0.217
Aa,Ab	±0.020	±0.010	±0.028	fixed	±7.9	±7.67	±8.2	±0.12	…	±0.034
2643/inner	0.27595	1997.1620	0.1986	…	…	113.4	…	12.493	…	(0.0)
Aa1,Aa2	±0.00002	±0.0012	±0.0073	…	…	±1.7	…	±0.109	…	…
101955/outer	38.6790	2016.110	0.118	0.855	127.6	233.4	87.40	2.66	…	−41.11
KUI 99 A,B	±0.031	±1.32	±0.016	±0.110	±0.08	±0.5	±0.05	±0.40	…	±0.08
101955/iner	2.51013	2000.518	0.6170	0.1242	147.1	109.7	24.1	3.27	6.93	0.457
BAG 14 Aa,Ab	±0.00052	±0.004	±0.0047	±0.0011	±1.8	±1.8	±1.7	±0.12	±0.71	±0.005
103987/outer	19.205	2006.259	0.1743	0.2195	102.8	17.6	65.1	4.005	9.58	−1.97
WSI 6 A,B	±0.080	±3.60	±0.0083	±0.0013	±0.5	±2.6	±1.0	±0.082	±0.22	±0.05
103987/inner	1.03483	2014.6223	0.0934	0.0284	97.3	124.9	68.6	9.528	…	0.350
DSG 6 Aa,Ab	±0.00008	±0.0089	±0.0040	fixed	±12.5	±3.1	±13.7	±0.058	…	±0.062
111805/outer	30.127	2010.179	0.324	0.3361	154.25	84.92	88.28	6.06	8.60	−22.58
HDO 295 B,A	±0.031	±0.073	±0.004	±0.0015	±0.09	±0.18	±0.10	±0.14	±0.23	±0.08
111805/iner	1.5012	1986.093	0.022	0.0385	334.5	232.9	85.80	13.13	19.21	−0.330
BAG 15 Ba,Bb	±0.0004	±0.093	±0.011	±0.0010	±1.0	±22.3	±1.6	±0.25	±3.1	±0.015

estimated from its absolute magnitude. The outer mass sum of 2.91 $\mathcal{M}_\odot$ leads to the dynamical parallax of 16.1 mas; the *Hipparcos* parallax of 17.5 mas is likely biased.

Taking the masses listed in Table 5, we convert them back to the V and K magnitudes using the same standard relations. It turns out that the spectroscopic secondaries Aa2 and Ab are indeed faint and do not influence the combined photometry. The modeled and measured combined K magnitudes are 6.26 and 6.35 mag, respectively, so the model reproduces the actual $V-K$ color reasonably well. The wobble factor $f=0.22$ leads to the mass ratio of 0.28 in the middle orbit, while the adopted masses imply $q=0.27$, in good agreement. If the innermost orbit had a small inclination, the mass of Aa2 would be larger, and the wobble factor would be smaller than measured.

Given the estimated masses, we evaluate the RV amplitudes in the outer orbit, $K_1=3.2\,\mathrm{km\,s^{-1}}$ and $K_2=6.9\,\mathrm{km\,s^{-1}}$. The free adjustment leads to the much smaller $K_1=1.4\,\mathrm{km\,s^{-1}}$. The RV of B in Figure 4 is a fake point added to show the expected RV curve for the visual secondary that is not actually measured. Blending with the lines of B likely explains the too small RV amplitude derived by the free fit to the RVs and increases the RV errors of Aa1, compared to a truly single star (rms residuals $0.56\,\mathrm{km\,s^{-1}}$). The RV residuals indeed correlate positively with the RV, as expected from the blending effect. The sign of the RV trend in the outer orbit establishes its correct node. New RV measurements would be helpful for a better definition of the outer orbit and of all the periods. The spectrum of B should be detectable because it contributes a 0.21 fraction of the combined light in the V band.

The inner period ratio is 17.57 ± 0.07, and the outer period ratio is 14.43 ± 0.28. The angle Φ between the middle and outer orbits is $25\overset{\circ}{.}4 \pm 8\overset{\circ}{.}5$. With such relative inclination, the orbit of Aa,Ab precesses, but does not experience the Kozai–Lidov cycles. The small eccentricity of all orbits supports indirectly the absence of such cycles and the approximate coplanarity of all orbits.

4. HIP 101955

This is a nearby (17 pc) triple system HD 196795 or GJ 795. It has extensive literature dedicated to it. The inner subsystem Aa,Ab was discovered by Duquennoy (1987; hereafter D87) using CORAVEL and later resolved for the first time by Balega et al. (2002). Malogolovets et al. (2007) presented a detailed study of this triple system. Unlike other systems featured here, the inner orbit has a substantial eccentricity and the two orbits have large mutual inclinations. Figure 5 displays the inner orbit, while Figure 6 shows the trajectory of A,B with the wobble. Only the speckle measures of A,B since 1981 are used to fit the two orbits jointly, with the outer period fixed to its value found by using all of the data. The semimajor axis of the wobble is 55.1 ± 0.6 mas. The weighted rms residuals for both A,B and Aa,Ab are ∼3 mas in position, 0.48 and $0.58\,\mathrm{km\,s^{-1}}$ for the RVs of Aa and Ab, respectively.

One spectrum of HIP 101955 has been taken with CHIRON in 2015 on JD 2457261. Its cross-correlation function (CCF) with the binary mask is an asymmetric blend that can be fitted by two Gaussians. The fainter component is in fact a blend of Ab and B because their RVs were close at that time. The ratio of the dip areas of Ab+B and Aa in the CCF is 0.50, or $\Delta m=0.75$ mag, matching roughly the resolved photometry (the system model predicts 0.45 mag). The rms widths of the CCF dips of Aa and Ab+B are 4.12 and $5.11\,\mathrm{km\,s^{-1}}$, respectively.

The RVs measured by Duquennoy are likely affected by blending (CORAVEL did not resolve the blends, except on two occasions). Owing to this, the "spectroscopic" masses of Aa and Ab derived from the combined inner orbit are too small (0.7 and 0.4 $\mathcal{M}_\odot$).

The system model starts with the combined $V=7.84$, the *Hipparcos* parallax, and the magnitude differences $\Delta V_{\mathrm{Aa,Ab}}=1.35$ mag (Malogolovets et al. 2007), $\Delta V_{\mathrm{A,B}}=1.35$ mag (*Hipparcos*). Individual magnitudes of the components and their estimated masses are listed in Table 5, leading to the mass sum of of 2.02 $\mathcal{M}_\odot$ for AB. The orbit of A,B matches this

Table 3
Relative Positions and Residuals (Fragment)

HIP	Sys	Date (year)	θ (°)	ρ (″)	σ (″)	O−C$_\theta$ (°)	O−C$_\rho$ (″)	Ref[a]
2643	A,B	1885.8100	121.2	0.5000	0.1000	−6.4	0.0055	M
2643	A,B	1948.7900	137.8	0.3400	0.1000	0.6	−0.0823	M
2643	A,B	1954.9800	130.1	0.4900	0.1000	1.5	0.0036	M

Note.
[a] G: DSSI at Gemini-N; H: *Hipparcos*; M: micrometer measures; S: speckle interferometry at SOAR; s: other speckle interferometry.

(This table is available in its entirety in machine-readable form.)

Table 4
Radial Velocity and Residuals (Fragment)

HIP	Comp	JD +2400000	RV	σ_{RV} (km s^{-1})	O−C	Ref[a]
2643	Aa1	48851.5080	6.940	0.490	−0.826	T
2643	Aa1	48947.3570	5.330	0.500	−0.884	L
2643	Aa1	49952.5990	−4.870	0.590	−0.703	L
2643	Aa1	48913.5800	−12.890	1.700	−1.497	L

Note.
[a] C: CHIRON; D: D87; L: CfA; L-: Cfa −1 km s^{-1}; T: Tokovinin & Smekhov (2002).

(This table is available in its entirety in machine-readable form.)

Table 5
Magnitudes and Masses

HIP	Comp.	V (mag)	$\mathcal{M}$ ($\mathcal{M}_\odot$)
2643	Aa1	7.97	1.22
	Aa2	(14.9)	(0.36)
	Ab	(14.5)	0.42
	B	9.60	0.91
101955	Aa	8.39	0.74
	Ab	9.74	0.62
	B	9.47	0.65
103987	Aa	7.46	1.15
	Ab	(12.5)	0.56
	B	9.62	0.67
111805	A	7.48	1.14
	Ba	7.98	1.03
	Bb	9.25	0.85

mass sum for a parallax of 59.0 mas, in excellent agreement with 58.8 mas determined by Söderhjelm (1999). The mass sum derived from the inner orbit is then 1.49 $\mathcal{M}_\odot$, while the model gives 1.36 $\mathcal{M}_\odot$. The model predicts the combined K magnitude of 4.62 mag, the observed one is 4.74 mag.

The adopted masses imply $q_{\rm Aa,Ab} = 0.84$ and match the wobble amplitude that corresponds to $q_{\rm Aa,Ab} = f/(1-f) = 0.84$. However, the spectroscopic inner mass ratio is 0.45; it is biased by the reduced RV amplitude of Aa and strongly contradicts the relative photometry of Aa,Ab. Even if the RV amplitudes in the inner orbit were measured reliably, its small inclination prevents good independent measurement of stellar masses and distance. The RVs of Aa also do not fit the outer orbit well due to blending with the other components Ab and B. The mass sum in the outer system corresponds to

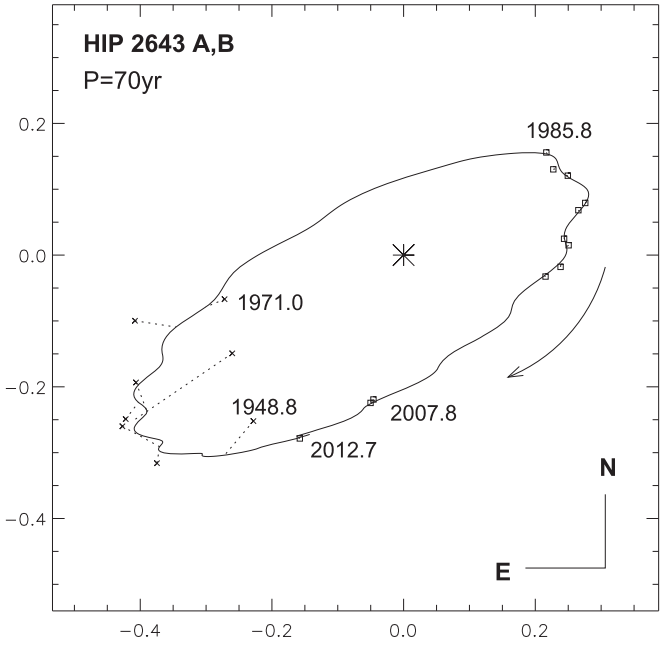

Figure 3. Orbit of HIP 2643 A,B in the sky. The primary component A is located at the coordinate origin (asterisk); the scale is in arcseconds. Squares and crosses denote relative positions of the secondary component B measured by speckle interferometry and micrometers, respectively; the short dotted lines connect the measurements to the calculated positions on the orbit. The wavy line is one complete orbit of the outer pair with the wobble.

$K_1 + K_2 = 11.2$ km s^{-1} (this is a robust estimate, given the high inclination), and the mass ratio $q_{\rm A,B}$ leads to the estimated amplitudes in the outer orbit $K_1 = 3.0$ and $K_2 = 8.2$ km s^{-1}. The fitted K_1 in the outer orbit converges to 2.66 km s^{-1}.

The period ratio is 15.41 ± 0.13, the angle between the orbital angular momenta is $\Phi = 64\overset{\circ}{.}8 \pm 1\overset{\circ}{.}4$. Strong interaction between the orbits and Kozai–Lidov cycles are expected (Xu et al. 2015). Malogolovets et al. (2007) estimated the period of these cycles to be 560 years and noted that they may be observable.

5. HIP 103987

HD 200580, alias G25-15, is a metal-poor ([Fe/H] ∼ −0.6) multiple system with a fast proper motion of 0.″46 per year. The single-lined spectroscopic orbit with a one-year period was published by Latham et al. (2002), while the outer system A,B was first resolved by Mason et al. (2001) in 1999 and is known as WSI 6. The astrometric orbit of the inner subsystem was published by Jancart et al. (2005). The inner pair Aa,Ab was resolved at Gemini, and its first visual orbit was published

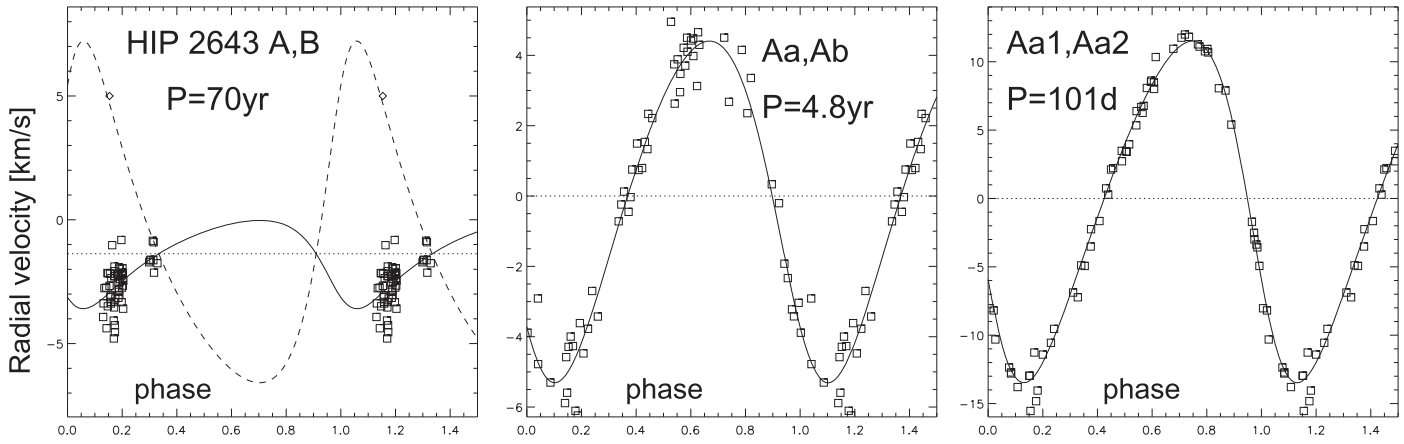

Figure 4. RV curves of HIP 2643. Left: outer orbit, middle: middle orbit, right: inner orbit. The full and dashed lines denote the curves for the primary and secondary components. The squares are the measured RVs where the motion in other orbits is subtracted. The diamond in the left-hand plot is a fake RV of the component B to illustrate the blending.

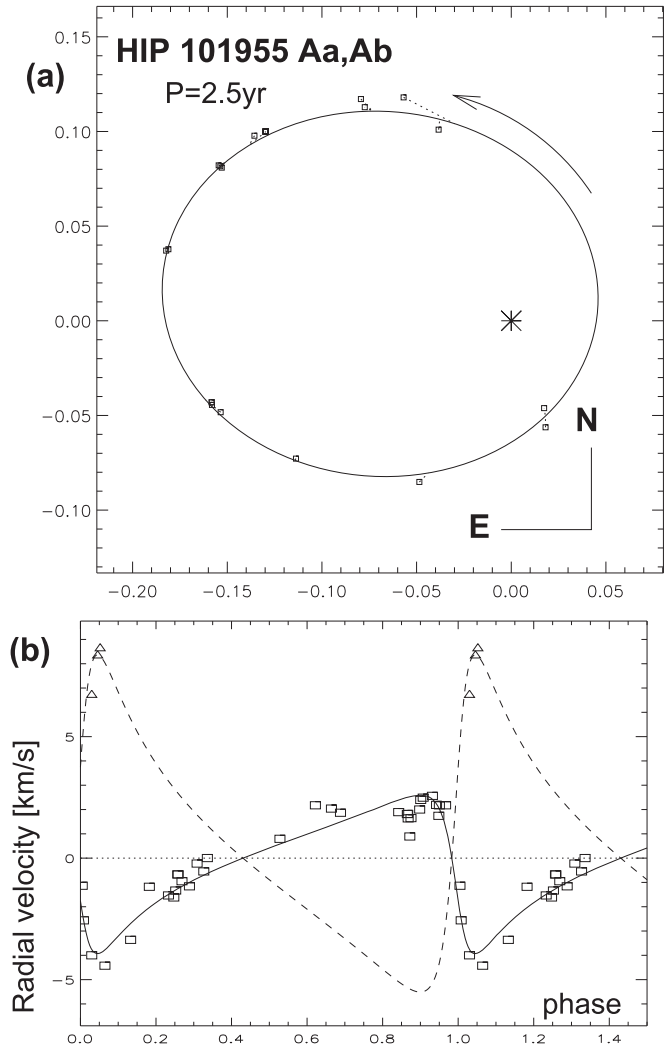

Figure 5. Inner orbit of HIP 101955 Aa,Ab. Top (a): orbit in the plane of the sky. Bottom (b): the RV curve with the outer orbit subtracted.

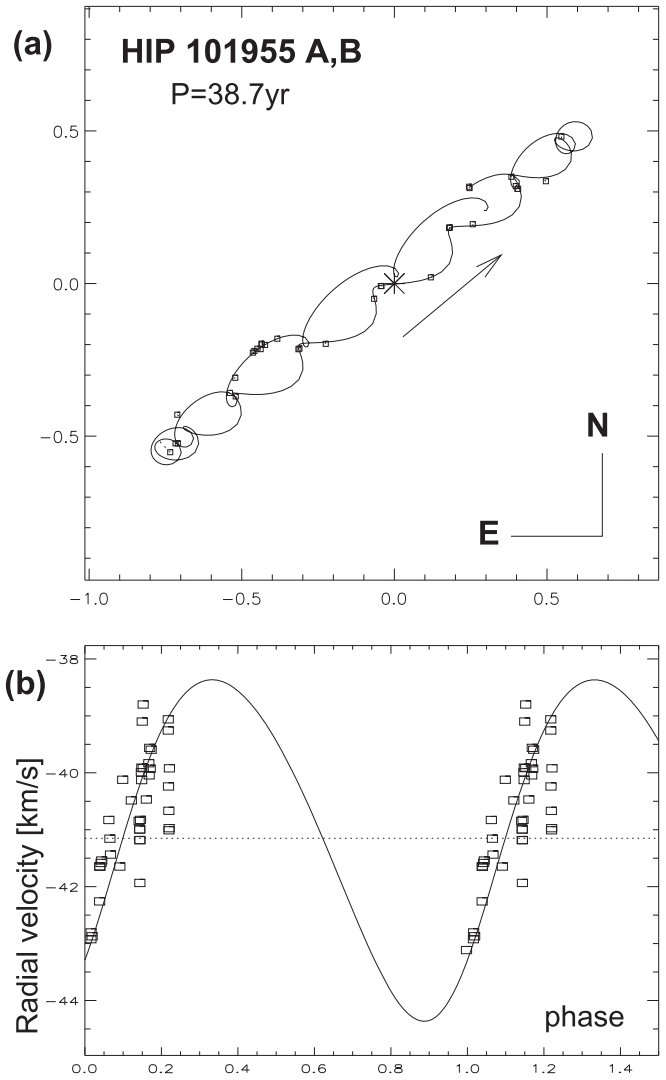

Figure 6. Outer orbit of HIP 101955 A,B. Top (a): orbit in the plane of the sky; only accurate speckle measures are plotted for one complete outer period. Bottom (b): the RV curve.

in H15. The available RVs now cover 1.5 outer periods and lead to the spectroscopic orbits of both inner and outer subsystems. The 19-year outer period found from the RVs matches well the visual orbit that almost covers the full ellipse; the preliminary 21 year orbit of A,B was published by Riddle et al. (2015). The pair A,B was observed at SOAR several times, but the inner subsystem has never been resolved.

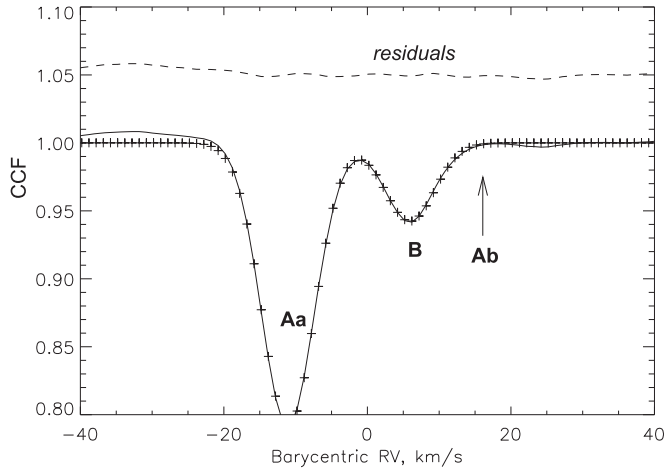

Figure 7. Cross-correlation function (CCF) of HIP 103987 on JD 2457301 and its approximation with two Gaussians (crosses). The residuals are plotted as a dashed line shifted to 1.05. The arrow marks the expected RV of the undetected component Ab.

In 2015, the star was observed twice with CHIRON in order to get fresh RVs and to detect the lines of other components. Indeed, the CCF of the spectrum and mask is double (Figure 7). Its components correspond to the visual primary Aa and the visual secondary B. There is no trace of Ab, which should have an RV of $+15\,\mathrm{km\,s^{-1}}$ at the moment of observation; the non-detection implies that Ab is at least ∼4 mag fainter than B and contradicts the speckle photometry in H15. Both CCF dips are very narrow and correspond to the axial rotation $V \sin i$ of 2.2 and $1.5\,\mathrm{km\,s^{-1}}$ for Aa and B, respectively. The ratio of the CCF areas corresponds to $\Delta m_{\mathrm{Aa,B}} = 1.43$ mag. At SOAR, we measured $\Delta y_{\mathrm{A,B}} = 2.17$ mag with the rms scatter of 0.05 mag. The spectroscopic Δm is underestimated because B has a lower effective temperature and stronger lines than Aa.

The speckle measures of A,B are accurate enough to detect the wobble caused by the subsystem Aa,Ab and to determine all of its orbital elements except a_1. Figures 8 and 9 show the inner and outer orbits. The weighted rms residuals to the measures of A,B in both coordinates are 1.3 and 2.5 mas, the wobble amplitude is 9.9 ± 1.8 mas. The astrometry has adequate phase coverage of the inner period mainly because the pair has been extensively monitored at SOAR during 2015 with the goal to resolve the Aa, Ab at quadratures, where the predicted separation reaches 20 mas. Most other measures of A,B are from Gemini and have an excellent accuracy of ∼1 mas. They were obtained at nearly the same phase of the inner orbit, as dictated by the Gemini time allocations. Joint analysis of the RVs and astrometry leads to the reliable inner orbit. The largest correlations are +0.5 between i_1 and f (which defines the astrometric amplitude) and −0.5 between i_1 and Ω_1. The wobble is detected at the 5.6σ significance level. To test the robustness of the relative orbit orientation, we fixed f to values of 0.29 and 0.41 (within $\pm\sigma$ of the nominal) and repeated the fits. In both cases, the angle Φ increased by 2°, less than its error.

The subsystem Aa,Ab was resolved at Gemini in four seasons (including the preliminary data of 2015 communicated by E. Horch). The separation was close to the diffraction limit of Gemini, hence the estimates of the separation and Δm are correlated. Probably for this reason, the $\Delta m_{\mathrm{Aa,Ab}} = 1.54$ mag at 692 nm published in H15 appears to be strongly underestimated (E. Horch, 2016, private communication) and contradicts both the lack of the spectroscopic detection of Ab

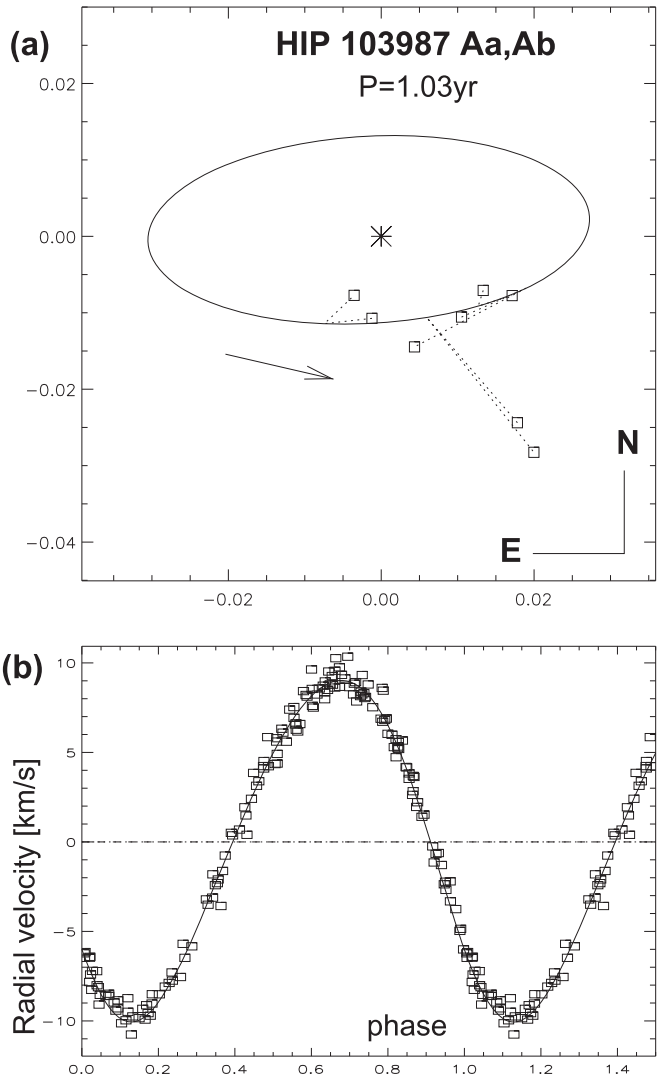

Figure 8. Orbit of HIP 103987 Aa,Ab in the plane of the sky (top, (a)) and the corresponding RV curve (bottom, (b)).

and its mass evaluated below. According to Figure 1 in H15 and $\Delta m_{\mathrm{Aa,Ab}} = 4.1$ mag at 692 nm estimated here, the subsystem should be undetectable. In all Gemini runs, the pair Aa,Ab was oriented in the north-south direction, where the atmospheric dispersion, which is not physically compensated in the DSSI speckle camera, could distort the measures. The prograde orbit of Aa,Ab computed in H15 from the resolved measures has a near-zero inclination, which contradicts the non-zero RV amplitude of Aa. This said, the positions of the inner pair measured at Gemini (Figure 8) roughly match its orbit, except the 2014 measures with nearly double separation. We question the resolved measures of the inner pair and use them in the combined orbital fit with very small weights.

The astrometric orbit of Aa,Ab by Jancart et al. (2005) has the expected semimajor axis of 10.4 mas, but corresponds to the retrograde motion ($i = 162°$) and has a very different $\Omega_{\mathrm{A}} = 15\overset{\circ}{.}6$ compared to our orbit. These authors have not revised the parallax, which is necessary for a one-year binary. Moreover, their results could be biased by the visual component B unresolved by *Hipparcos*. Therefore, this astrometric orbit should be ignored.

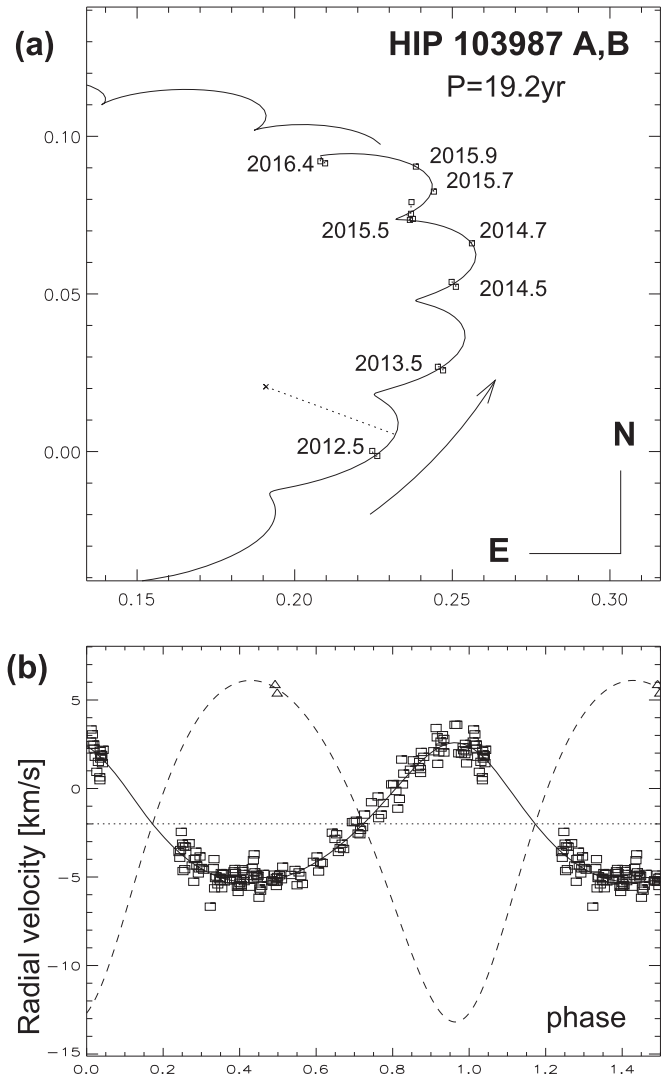

Figure 9. Orbit of HIP 103987 A,B (WSI 6) in the plane of the sky (a), where only a fragment of the full orbit is shown to highlight the wobble, and the RV curve (b), with squares for RV(Aa) and triangles for RV(B).

Owing to the RV(B) measured with CHIRON, the combined orbit of A,B yields the orbital parallax of 23.4 ± 0.3 mas and the components' masses 1.62 ± 0.09 $\mathcal{M}_\odot$ for A and 0.67 ± 0.06 $\mathcal{M}_\odot$ for B. However, the orbital masses are proportional to the cube of the RV amplitudes, and if the amplitudes are slightly reduced by the line blending with other components, the orbital masses are underestimated. The *Hipparcos* parallax of 19.3 mas is evidently biased by the one-year wobble.

We adopt the masses of 1.15, 0.56, and 0.67 $\mathcal{M}_\odot$ for Aa,Ab, and B, respectively, based on the system model. They correspond to the mass sum of 2.38 $\mathcal{M}_\odot$, slightly larger than measured, and the dynamical parallax of 23.2 mas, matching the orbital parallax within its error. The inner semimajor axis $a_{\rm Aa,Ab} = 28.4$ mas is then computed and fixed (remember that the resolved measures of Aa,Ab are questionable, while the wobble amplitude is determined by the fitted factor f).

The inner mass ratio $q_{\rm Aa,Ab} = 0.49$ matches the measured wobble amplitude. The spectroscopic mass of Ab calculated from the inner RV amplitude and inclination is 0.49 $\mathcal{M}_\odot$. Agreement with the adopted mass of Ab would be reached by a 4% increase of K_1 or for the inner inclination of 55° instead of the measured 69° ± 14°. If Ab is a normal M-type dwarf, we expect $\Delta m_{\rm Aa,Ab} = 4.1$ mag at 692 nm, much larger than $\Delta m_{\rm Aa,Ab} = 1.5$ mag measured at Gemini and in agreement with the spectroscopic non-detection of Ab with CHIRON. Alternatively, Ab could be a white dwarf.

The components' magnitudes listed in Table 5 are computed by using $\Delta V_{\rm AB} = 2.13$ mag measured by speckle interferometry at SOAR and by further assuming that $\Delta V_{\rm Aa,Ab} = 5$ mag to match the adopted mass of Ab. The model reproduces the combined K magnitude and predicts $V - K = 1.63$ mag; the actual $V - K = 1.52$ mag is slightly bluer, as it should be for a low-metallicity star. The outer and inner orbits are inclined by $\Phi = 6° \pm 9°$, i.e., they are almost coplanar. The period ratio is 18.55 ± 0.08.

6. HIP 111805

This system, HD 214608, is also metal-poor; it was studied in H15. The subsystem Ba,Bb, first resolved by Balega et al. (2002), belongs to the secondary component of the well-studied visual pair HDO 295 (ADS 16138) known since 1887. Both orbits are seen nearly edge-on and, as shown below, are well aligned, $\Phi = 2\overset{\circ}{.}5 \pm 1\overset{\circ}{.}5$. For this reason, the wobble is not obvious in the outer orbit plot. Most speckle observations did not resolve the inner pair Ba,Bb, which has fewer speckle measures compared to A,B.

The spectroscopic orbits of both subsystems were determined by Duquennoy (1987). Additional RVs obtained by D. L. are used here. They were derived by TODCOR and refer to the two brightest components A and Ba. The components often blend; therefore, several highly deviant RVs were discarded in the orbit calculation. In H15, the authors adopted the SB elements by Duquennoy and fitted only the remaining elements to the outer orbit. However, Duquennoy fixed the period of A,B using its older visual orbit, not spectroscopy. The combined orbit computed here uses all the data and removes this inconsistency.

The "primary" components are Ba and Bb, the "tertiary" is A (to get the orbit of B around A, change the outer elements $\Omega_{\rm A}$ and $\omega_{\rm A}$ d by 180°), the wobble coefficient $f = -0.33$ is negative. In the last iteration, we fixed the outer period and used only the speckle data for A,B in fitting the remaining 19 free parameters. As can be seen in Figures 10 and 11, the RV curves are rather noisy owing to the line blending. The weighted rms RV residuals are 0.97, 3.5, and 0.78 km s^{-1} for Ba,Bb, and A, respectively (with some outliers removed or given low weight). Only two uncertain measures of RV(Bb) by Duquennoy define the inner amplitude K_2. The rms residuals of the positional measures are from 3 to 5 mas in X and Y, for both orbits.

The *Hipparcos* parallax of 26.2 ± 0.6 mas gives a too small mass sum of 2.3 $\mathcal{M}_\odot$ for the well-defined outer orbit. We adopt the orbital parallax of 24.1 mas derived from the combined orbit of A,B and the mass sum of 3.0 $\mathcal{M}_\odot$, in agreement with the model masses. The mass sum in the inner orbit is 1.82 $\mathcal{M}_\odot$ and, by subtraction, the mass of A is 1.18 $\mathcal{M}_\odot$. It matches the inner RV amplitudes, but the large error of K_2 makes the $M \sin^3 i$ estimate in the inner orbit quite uncertain.

H15 derived the masses of A,Ba, and Bb as 1.12, 0.92, and 0.77 $\mathcal{M}_\odot$ using standard relations and disregarding the low metallicity. The corresponding spectral types are F9V, G5V, and K1V. We repeated the modeling assuming the orbital parallax of 24.1 mas. The relative photometry is $\Delta V_{\rm A,B} = 0.50$ mag, based on the *Hipparcos* datum and some measurements by Horch,

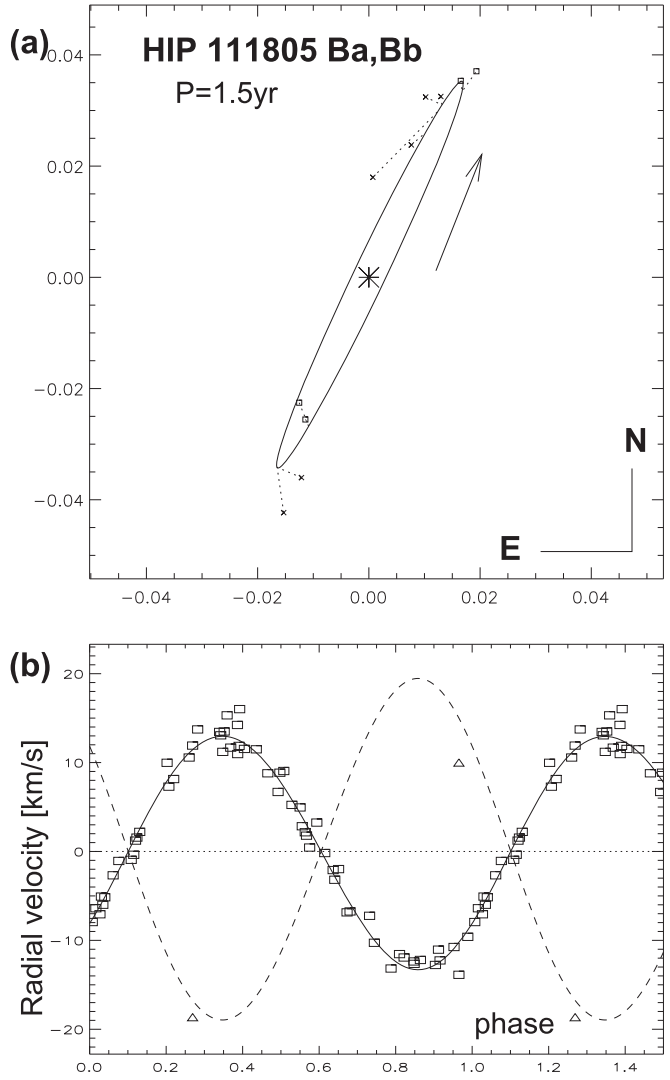

Figure 10. Orbit of HIP 111805 Ba,Bb (BAG 15). Top (a): orbit in the sky; the measures at Gemini are plotted as squares, the remaining measures as crosses. Bottom (b): the RV curve (squares for Ba and triangles for Bb).

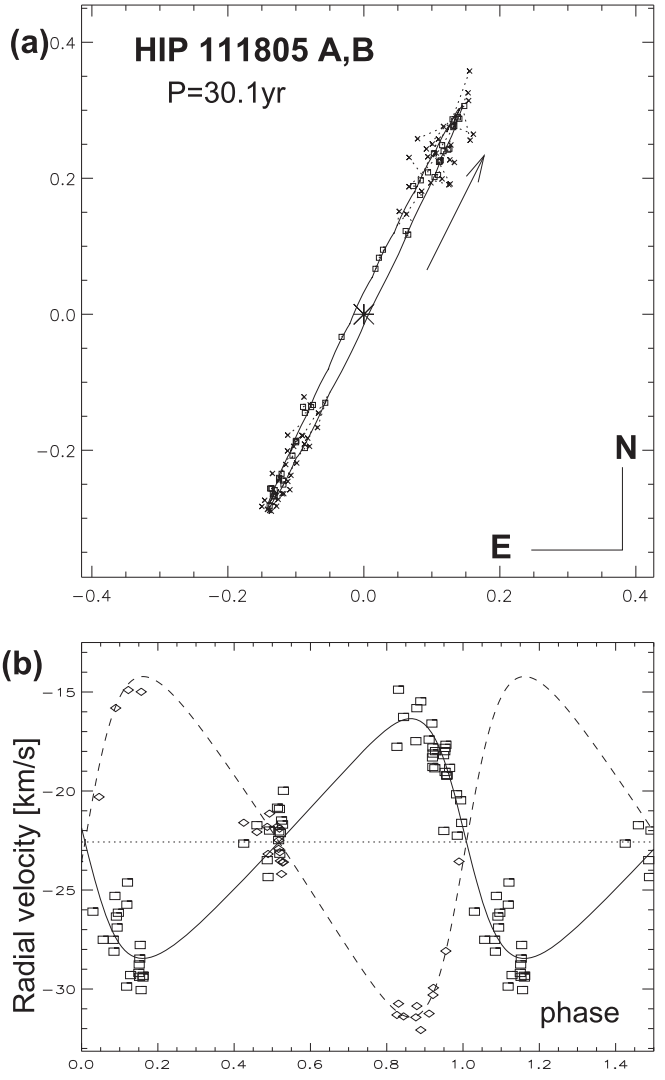

Figure 11. Orbit of HIP 111805 A,B (HDO 295). Top (a): orbit in the sky. Bottom (b): the RV curve (squares for Ba and diamonds for A).

while $\Delta V_{\rm Ba,Bb} = 1.27$ mag is measured by Balega et al. The derived masses are 1.14, 1.03, and 0.85 $\mathcal{M}_\odot$, or the mass sum of 3.02 $\mathcal{M}_\odot$. The combined K magnitude of the model is 5.25, the observed one is 5.31 mag. The model matches both orbits quite well.

The model implies $q_{\rm Ba,Bb} = 0.83$. The measured wobble factor $f^* = -0.33$ (most measures of A,B refer to the photocenter of B) corresponds to $q_{\rm Ba,Bb} \approx 0.60$, and the uncertain inner spectroscopic mass ratio is $q_{\rm Ba,Bb} \approx 0.68$. It is possible that the component Bb is less massive and fainter than deduced from the photometric model.

7. Summary and Discussion

We determined inner and outer orbits in four multiple systems using both resolved measures and RVs. The ascending nodes are therefore identified without ambiguity, allowing us to calculate the angle Φ between the orbital angular momentum vectors. These angles, period ratios, outer periods $P_{\rm out}$ and outer eccentricities $e_{\rm out}$ are listed in Table 6. In three systems, the orbits are approximately co-aligned, and both inner and outer eccentricities are small. In such cases, the inner orbits precess around the total angular momentum, with Φ being approximately constant. Only in HIP 101955, the orbits are closer to perpendicularity than to alignment, $\Phi = 65°$. In this configuration, the angle Φ and the inner eccentricity oscillate in the so-called Kozai–Lidov cycles. Indeed, the inner eccentricity in HIP 101955 is large, $e = 0.61$. None of the four close multiple systems are conter-rotating (all have $\Phi < 90°$), in line with the general trend of orbit co-alignment noted by Sterzik & Tokovinin (2002). The massive counter-rotating close triple σ Ori with $\Phi \sim 120°$ (Schaefer et al. 2016) could be formed by a different process.

Table 6
Relative Orbit Orientation and Period Ratio

HIP	$P_{\rm out}$ (year)	$e_{\rm out}$	$P_{\rm out}/P_{\rm in}$	Φ (°)
2643	70.34	0.33	14.43 ± 0.28	25.4 ± 8.5
2643	4.85	0.14	17.57 ± 0.07	…
101955	38.68	0.12	15.41 ± 0.13	64.8 ± 1.4
103987	19.20	0.17	18.55 ± 0.08	6.2 ± 9.0
111805	30.13	0.32	20.07 ± 0.02	2.5 ± 1.5

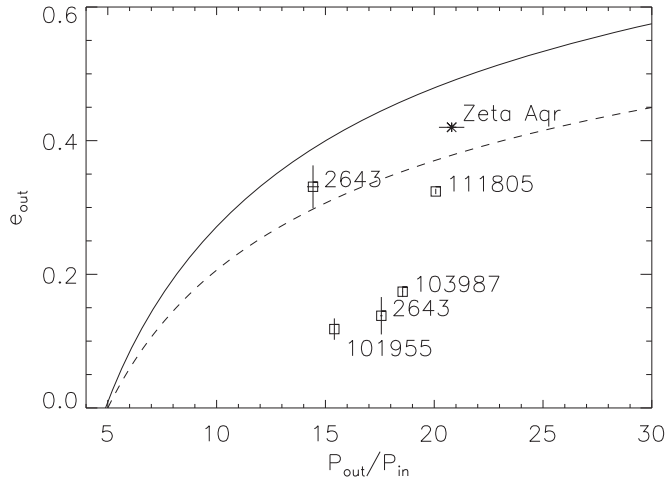

Figure 12. Period ratio and outer eccentricity. The full and dashed lines are the dynamical stability criteria by Mardling & Aarseth (2001) and Tokovinin (2004), respectively.

Figure 12 compares the period ratios and outer eccentricities of the multiple systems studied here with the dynamical stability criterion of Mardling & Aarseth (2001). The outer orbit in HIP 2643, as well as ζ Aqr (Tokovinin 2016b), do not satisfy the more strict empirical criterion of Tokovinin (2004), which therefore is not valid.

The quadruple system HIP 2643 with a 3+1 architecture resembles the "planetary" quadruple HD 91962 (Tokovinin et al. 2015) in several ways. In both multiple systems, all three orbits have moderate eccentricities, the outer and middle orbits are not far from coplanarity, and the period ratios between the hierarchical levels are small. This suggests that there was some interaction between the orbits, at least during the formation of these systems. However, the ratio of the two inner periods in HD 91962 is 19.0, suggesting a mean motion resonance, while it is not integer in HIP 2643.

Some data used in this work were obtained at the Southern Astrophysical Research (SOAR) telescope. We thank E. Horch for critical re-evaluation of the Gemini speckle data and communication of his unpublished observations of HIP 103987. We also thank both referees for a careful and inquisitive check of the manuscript.

This work used the SIMBAD service operated by Centre des Données Stellaires (Strasbourg, France), bibliographic references from the Astrophysics Data System maintained by SAO/NASA, data products of the Two Micron All-sky Survey (2MASS), and the Washington Double Star Catalog maintained at USNO.

Facilities: ORO:Wyeth (CfA Digital Speedometer), FLWO:1.5 m (CfA Digital Speedometer, TRES), SOAR (HRcam), CTIO:1.5 m (CHIRON).

References

Albrecht, S., Winn, J. N., Torres, G., et al. 2014, ApJ, 785, 83
Balega, I. I., Balega, Y. Y., Hofmann, K.-H., et al. 2002, A&A, 385, 87
Duquennoy, A. 1987, A&A, 178, 114 (D87)
Fabrycky, D. C., Lissauer, J. J., Ragozzine, D., et al. 2014, ApJ, 790, 146
Hartkopf, W. I., Mason, B. D., & Worley, C. E. 2001, AJ, 122, 3472 (VB6)
Horch, E. P., van Altena, W. F., Demarque, P., et al. 2015, AJ, 149, 151 (H15)
Jancart, S., Jorissen, A., Babusiaux, C., & Pourbaix, D. 2005, A&A, 442, 365
Kervella, P., Mérand, A., Petr-Gotzens, M. G., et al. 2013, A&A, 552, 18
Latham, D. W. 1985, in IAU Coll. 88, Stellar Radial Velocities, ed. A. G. D. Philip & D. W. Latham (Schenectady: L. Davis Press), 21
Latham, D. W. 1992, in ASP Conf. Ser. 32, IAU Coll. 135, Complementary Approaches to Binary and Multiple Star Research, ed. H. McAlister & W. Hartkopf (San Francisco: ASP), 110
Latham, D. W., Stefanik, R. P., Torres, G., et al. 2002, AJ, 124, 1144
Malogolovets, E. V., Balega, Y. Y, & Rastegaev, D. A. 2007, AstBu, 62, 111
Mardling, R. A., & Aarseth, S. J. 2001, MNRAS, 321, 398
Mason, B., Hartkopf, W. I., Holdenried, E. R., & Rafferty, T. J. 2001, AJ, 121, 3224
Mason, B. D., & Hartkopf, W. I. 2014, IAUDS, 183, 1
McArthur, B. E., Benedict, G. F., Barnes, R., et al. 2010, ApJ, 715, 1203
Riddle, R. L., Tokovinin, A., Mason, B. D., et al. 2015, ApJ, 799, 4
Schaefer, G. H., Hummel, C. A., Gies, D. R., et al. 2016, AJ, 252, 213
Söderhjelm, S. 1999, A&A, 341, 121
Sterzik, M., & Tokovinin, A. 2002, A&A, 384, 1030
Szentgyorgyi, A. H., & Furész, G. 2007, RMxAA, 28, 129
Tokovinin, A. 2004, RMxAA, 21, 7
Tokovinin, A. 2014, AJ, 147, 86
Tokovinin, A. 2016a, AJ, 152, 11
Tokovinin, A. 2016b, ApJ, 831, 151
Tokovinin, A., Fischer, D. A., Bonati, M., et al. 2013, PASP, 125, 1336
Tokovinin, A., Latham, D. W., & Mason, B. D. 2015, AJ, 149, 195
Tokovinin, A., Mason, B. D., Hartkopf, W. I., et al. 2016, AJ, 151, 153
Tokovinin, A. A., & Smekhov, M. G. 2002, A&A, 382, 118
van Leeuwen, F. 2007, A&A, 474, 653
Xu, X.-B., Xia, F., & Fu, Y.-N. 2015, RAA, 15, 1857
Zhu, L.-Y., Zhou, X., Hu, J.-Y., et al. 2016, AJ, 151, 107